applied sciences

MDPI

Article

Voltammetric Study for the Determination of Diclofenac in Aqueous Solutions Using Electro-Activated Carbon Electrodes

Silvia Berto [1,*], Enrico Cagno [1], Enrico Prenesti [1], Giulia Aragona [1], Stefano Bertinetti [1], Agnese Giacomino [2], Paolo Inaudi [2], Mery Malandrino [1], Emanuele Terranova [1] and Ornella Abollino [2]

[1] Department of Chemistry, University of Turin, Via P. Giuria 7, 10125 Turin, Italy
[2] Department of Drug Science and Technology, University of Turin, Via P. Giuria 9, 10125 Turin, Italy
* Correspondence: silvia.berto@unito.it

Featured Application: The knowledge acquired in this work on the diclofenac electrochemical behavior will be essential to develop a voltammetric sensor for the drug detection in water samples.

Abstract: Diclofenac (DCF) is a nonsteroidal anti-inflammatory drug to treat pain and inflammatory diseases. The high consumption of the drug leads to a significant change in the ecosystem. With the aim of optimizing a fast screening analysis for DCF detection on many samples with a sensitive and cheap procedure, we considered electrochemical methods using carbon-based electrodes as sensors. The electrochemical behavior of the DCF was studied on glassy carbon electrodes (GCE) and on screen-printed carbon electrodes (SPCEs) from two different suppliers after an anodic activation. The surface of the SPCEs was analyzed by scanning electron microscope (SEM) and Energy Dispersive Spectrometry (EDS). On all the activated electrodes, the voltammetric procedure (Differential Pulse Voltammetry) for the determination of DCF was optimized by the Experimental Design method, and the linearity range of the response, as well as the calibration and limit parameters (limits of detection—LoD; limit of quantification—LoQ), were defined. Analyses on SPCEs were performed both by immersing the electrode in the solution and by deposing a drop of solution on the electrode. DCF signals are stabilized by the polishing process and enhanced by the anodic activation and acid pH. The electrochemical response of DCF is not reversible, and its by-products tend to be adsorbed on the surfaces, particularly on GCE. The lowest limit parameters were obtained using the GCE (LoD = 1.6 μg L^{-1}) and the SPCE, having the smallest surface, immersed in solution (LoD = 7 μg L^{-1}).

Keywords: diclofenac; glassy carbon electrode; screen printed electrodes; voltammetry; electrochemical activation; natural surface waters

Citation: Berto, S.; Cagno, E.; Prenesti, E.; Aragona, G.; Bertinetti, S.; Giacomino, A.; Inaudi, P.; Malandrino, M.; Terranova, E.; Abollino, O. Voltammetric Study for the Determination of Diclofenac in Aqueous Solutions Using Electro-Activated Carbon Electrodes. *Appl. Sci.* **2022**, *12*, 7983. https://doi.org/10.3390/app12167983

Academic Editor: Carmen Zaharia

Received: 14 July 2022
Accepted: 7 August 2022
Published: 9 August 2022

1. Introduction

Diclofenac (2-[(2,6-dichlorophenyl)amino]benzeneacetic acid sodium salt; CAS Number: 15307-79-6; hereafter, DCF) is a nonsteroidal anti-inflammatory drug (NSAID) with high activity and considerable tolerability. It is widely used throughout the world as a pain and inflammation reliever. Some studies, based on Intercontinental Marketing Services (IMS) health data (which serves 82% of the global population), estimated annual global consumption to be 1443 ± 58 tons [1] of the molecule. Additionally, this amount could probably be underestimated because it did not take into account the consumption for veterinary purposes. This high consumption leads to the subsequent input of the drug into the ecosystem. After use, DCF is partially released into wastewater, and the efficiency of DCF removal by wastewater treatment plants (WWTPs) is not very high. Studies on the elimination rates during the WWTPs process indicate removal rates for DCF ranging between 0 and 80%, but more frequently, the rates are between 20 and 40% [2]. Consequently, DCF was detected in different environmental compartments. The technical report

published in 2018 by the European Joint Research Centre [3] showed a detection frequency of DCF above 50% and a mean concentration value of the drug equal to 66 ng L^{-1}. These values were estimated by analyzing 6698 samples of surface water collected at 607 sites across 25 European Countries. Moreover, a direct eco-toxicological effect of DCF residues in wildlife was documented [4,5] and, based on the results collected during the monitoring program of the EU [3], the estimated Predicted No Effect Concentration (PNEC) for DCF was lowered from 0.1 to 0.05 ng L^{-1}.

The fast detection of DCF in the effluent of WWTPs, surface water, or in any type of natural water sample would allow for an estimation of the drug contamination level, which could help immediate decision-making. The suggested analytical method to detect DCF in water samples is Liquid Chromatography coupled with Mass Spectrometry after the treatment of the sample with Solid Phase Extraction (SPE-LC-MS-MS) [6,7]. These techniques are expensive and time-consuming; moreover, they need highly qualified staff and qualified maintenance service of the instruments and can neither be performed in the field after sampling nor directly in the stream. In order to allow a fast screening analysis on many samples with a sensitive and cheap procedure, these techniques are unsuitable, whereas electrochemistry could be a good solution thanks to its low cost, high sensitivity, and potential portability. Several research papers report on the application of electrochemical methods for the quantification of DCF using, in particular, carbon-based electrodes [8–19] (see Table 1). Most of these applications use carbon electrodes modified by the application of materials that enhance electron transfer, such as ionic liquids, carbon nanotubes, and silica nanoparticles. More simply, in this work, an electro-activation method was tested. The procedure was applied in previous works to increase the signal of paracetamol on glassy carbon electrodes (GCEs) and required the application of an anodic potential for a defined time, with the electrode surface immersed in a borate-phosphate buffer solution at pH 9 [20,21]. As reported in previous work [20], the application of this procedure to GCEs leads to the formation of a homogenous and perfectly adherent layer four times less resistive than the original surface. Since the interesting results were obtained with paracetamol, the effect of the same activation process was applied to the voltammetric detection of DCF. The electrochemical behavior of DCF was studied on both GCE and screen-printed carbon electrodes (SPCEs) after the anodic activation. The surface of the SPCEs was analyzed by Scanning Electron Microscopy (SEM) and Energy Dispersive Spectrometry (EDS). On both the activated carbon-based electrodes, the voltammetric procedure (Differential Pulse Voltammetry, DPV) for the determination of DCF was optimized by a Design of Experimental (DoE) approach, and the linearity range of the response as well as the calibration and limit parameters (limits of detection–LoD; limit of quantification–LoQ) were defined.

Table 1. Analytical performance of electrochemical methods previously developed for the quantification of diclofenac using carbon-based electrodes.

Electrode [1]	Linear Range (μmol L^{-1})	Detection Limit (μmol L^{-1}/μg L^{-1})	Reference
EPPGE	0.01–1	0.0062/1.8	[8]
MWCNTs/$Cu(OH)_2$NP/ILNC/GCE	0.18–119	0.04/11.8	[9]
VFMCNTPE	5–600	2.0/592.3	[10]
IL/CNTPE	0.5–300	0.2/59.2	[11]
MWCNT–IL|CCE	0.05–50	0.018/5.3	[12]
IL/CNTPE	0.3–750	0.09/26.7	[13]
MWCNTs/PGE	0.047–12.95	0.017/5.0	[14]
Cu/CTS/MWCNTs/GCE	0.3–200	0.021/6.2	[15]
Silica NPs-CPE	0.1–500	0.046/13.6	[16]
SPCE-CeO_2 NP	0.4–26	0.4/118.5	[17]
SPCE/MWCNTs-COOH	0.0001–0.020	0.00003/0.01	[18,19]

Table 1. *Cont.*

Electrode [1]	Linear Range (μmol L^{-1})	Detection Limit (μmol L^{-1}/μg L^{-1})	Reference
GCE-anodic act	0.01–0.05	0.0053/1.6	This work
SPCE-anodic act	0.067–0.49	0.024/7.0	This work

[1] EPPGE = edge plane pyrolytic graphite electrode; MWCNTs/$Cu(OH)_2$NP/ILNC/GCE = multiwalled carbon nanotubes/$Cu(OH)_2$ nanoparticles/ionic liquid nanocompounds (1-ethyl-3-methylimidazolium hexafluorophosphate) modified glassy carbon electrode; VFMCNTPE = vinylferrocene modified multiwall carbon nanotubes paste electrode; IL/CNTPE = ionic liquid-modified carbon nanotubes paste electrode; MWCNT–IL|CCE = multiwalled carbon nanotube and ionic liquid modified carbon ceramic electrode (MWCNT–IL|CCE); IL/CNTPE = 1-butyl-3-methylimidazolium hexafluoro phosphate modified carbon nanotubes paste electrode; MWCNTs/PGE = multiwalled carbon nanotubes modified pencil graphite electrode; Cu/CTS/MWCNTs/GCE = chitosan–copper complex multiwalled carbon nanotubes modified glassy carbon electrode; Silica NPs-CPE = Silica nanoparticles modified carbon paste electrode; SPCE-CeO_2 NP = CeO_2 nanoparticle modified screen-printed carbon electrodes; SPCE/MWCNTs-COOH = screen-printed carbon electrode modified with carboxyl functionalized multiwalled carbon nanotubes; G/SPE = graphene nanoribbon modified screen printed electrode; GCE-anodic act = Glassy Carbon Electrode after anodic activation; SPCE-anodic act: screen-printed carbon electrode after anodic activation.

2. Materials and Methods

2.1. Reagents

Diclofenac, purity >98%; acetaminophen, purity >99%; potassium dihydrogen phosphate, purity >99%; sodium tetraborate, purity >99%; potassium chloride, purity >99%; sodium hydroxide pellets; 37% hydrochloric acid; 85% ortho-phosphoric acid; acetic acid, purity >99%; acetonitrile, purity ≥99.9%; ethanol, purity ≥99.8%, were purchased from Sigma Aldrich–Merck (Darmstadt, Germany).

Ultra-pure water was produced by a Milli-Q system (resistivity of 18 MΩ cm). The DCF stock solution was weekly prepared in acetonitrile. The borate-phosphate buffer (hereafter, BPB solution) was prepared by dissolving KH_2PO_4 and $Na_2B_4O_7$ salts in Milli-Q water to respective final concentrations of 4.5×10^{-2} and 0.5×10^{-2} mol L^{-1}, or 4.5×10^{-1} and 0.5×10^{-1} mol L^{-1}, and by adjusting the pH value to 9.0 with a concentrated aqueous solution of sodium hydroxide. The phosphate buffer at pH 7.0 was prepared by dissolving KH_2PO_4 in Milli-Q water to a final concentration of 2.5×10^{-2} mol L^{-1} and by adjusting the pH value with a concentrated aqueous solution of sodium hydroxide. The phosphate buffer at pH 2.0 was prepared in two different ways: by dissolving KH_2PO_4 in Milli-Q water to a final concentration of 2.5×10^{-2} mol L^{-1} and by adjusting the pH value with H_3PO_4 or by dissolving KH_2PO_4 in Milli-Q to a final concentration of 1.0×10^{-2} mol L^{-1} and by adjusting the pH with HCl. The acetate buffer at pH 4.7 was prepared by dissolving concentrated acetic acid in Milli-Q water to a final concentration of 2.5×10^{-2} mol L^{-1} and by adjusting the pH with a concentrated aqueous solution of sodium hydroxide.

The phosphate buffer at pH 2.0 for the SPCE measurements was prepared by dissolving KH_2PO_4 in Milli-Q water to a final concentration of 1.0×10^{-1} mol L^{-1} and by adjusting the pH value with 1.0 mol L^{-1} HCl aqueous solution.

2.2. Apparatuses

The electrochemical measurements were carried out with a PalmSens4 potentiostat (purchased from Thasar Srl, Milan, Italy), controlled by the PSTrace v5.8 software, and connected with an IKA-Topolino magnetic stirrer. The electrochemical cells were composed of a common three-electrode system or screen-printed electrodes. The configuration of the three-electrode system was: a Glassy Carbon Electrode (GCE) with a surface diameter of 3 mm (purchased from ALS Co., Ltd., Tokyo, Japan) as a working electrode; a platinum wire (0.5 mm, surface area ~0.7 cm^2) as a counter electrode, and an RE-1B Ag/AgCl, 3 mol L^{-1} KCl (ALS Co., Ltd.), as a reference electrode. The screen-printed electrodes, BTV-SPCEs (model AC1.W4.R1, henceforth SPCE1), and DropSens SPCEs (model C11L, henceforth SPCE2) were purchased from BVT Technologies (Czech Republic) and by Metrohm (Italiana Srl, Origgio (VA), Italy), respectively. The working, the reference, and the auxiliary electrodes are applied on a corundum ceramic base. The working electrode was made of

carbon and had a diameter of 1 mm (SPCE1) and 4 mm (SPCE2), the reference electrode was made of Ag/AgCl (mixing ratio 60/40), and the counter electrode was made of carbon (SPCE1) or graphite (SPCE2). The SPEs were connected through a PalmSens SPE connector (purchased from Thasar Srl) with 3 banana receptacles (2 mm) and a connection for the screen-printed electrodes (maximum thickness of 0.5 mm).

The solution pH was measured by the Metrohm, mod. 713 potentiometer (resolution of ±0.1 mV) coupled with a Metrohm combined glass electrode (mod. 6.0259.100), with Ag/AgCl/3M KCl internal reference).

For the characterization of the surface of the SPCEs, the Field Emission Scanning Electron Microscope-FE-SEM-TESCAN (Kohoutovice, Czech Republic) S9000G was used.

2.3. Procedures

2.3.1. Polishing

The electrode surface was prepared before use by rubbing it for a minute on a polishing pad wetted by an alumina–water dough (diameter of alumina granules: 0.3 µm; purchased from ALS Co., Ltd. ALS), then rubbing it for a minute on a polishing pad wetted by deionized water. Finally, it was thoroughly washed with ethanol and deionized water for GCE and only deionized water for SPCEs.

2.3.2. Electrochemical Activation

As reported by Chiavazza et al. [20], the activation of the GCE consisted of the application of a 2.0 V anodic potential for 60 s under magnetic stirring (500 rpm) to the GCE immersed in a 5.0×10^{-2} mol L^{-1} BPB solution. The activation was monitored by chronoamperometry (CA) using the following parameters: time for equilibration: 5 s; applied potential: 2.0 V; interval time: 0.5 s; run time: 60 s. Before processing the samples, about ten voltammetric scans on a blank solution were performed to stabilize the signal. The activated electrode (aGCE) was then directly used for the measurements.

The activation procedure applied to SPCEs was optimized in this work on the paracetamol signals. The SPCEs were immersed in the 5.0×10^{-1} mol L^{-1} BPB solution at pH = 9, and CA was applied with the following parameters: time for equilibration: 10 s; applied potential: 1.3 V; interval time: 0.1 s; run time: 60 s. No stirring was applied. The activated SPCE (aSPCE) was then carefully washed and used for the measurements. Before processing the samples, about five voltammetric scans on a blank solution were performed to stabilize the signal.

2.3.3. Electrochemical Measurements

Cyclic Voltammetry

The Cyclic Voltammetry (CV) measurements were carried out by GCE and aGCE and by SPCE and aSPCE to study the DCF electrochemical behavior. With the aGCEs, the following measurement parameters were used: time for equilibration: 15 s; potential step: 5.0 mV; potential range: 0.0–0.9 V; scan rate: 0.02–0.175 V s^{-1}. The CV signals were recorded on solution $7 \cdot 10^{-8}$ mol L^{-1} DCF at different pH and medium: pH 2.0, with 1×10^{-2} mol L^{-1} hydrochloric acid; pH 2.0, with 2.5×10^{-2} mol L^{-1} phosphoric acid; pH 4.7, with 2.5×10^{-2} mol L^{-1} acetic buffer; pH 7.0, with 2.5×10^{-2} mol L^{-1} phosphate buffer.

With the aSPCE, the following measurement parameters were used: time for equilibration: 30 s; potential step: 5 mV; potential range: 0.0–0.9 V; scan rate: 0.05 V s^{-1}. The CV signals were collected on solutions of DCF at different concentrations (in the range 3.3×10^{-6}–8.2×10^{-6} mol L^{-1}) kept at pH 2.0 with 1.0×10^{-1} mol L^{-1} phosphate buffer.

Differential Pulse Voltammetry

Differential Pulse Voltammetry (DPV) was applied using both aGCE and aSPCE.

The electrochemical experiments were carried out at room temperature. The potential scan was carried out between 0.0 and 1.0 or 0.1 and 0.6 V with a step height (E_{step}) of 5 mV

for aGCE and of 4 mV for aSPCE. The other DPV parameters were optimized by a Design of Experiments (DoE) approach for both aGCE and aSPCEs, as described below.

2.4. Design of Experiment (DoE)

In order to maximize the sensitivity of the DPV measurements, a DoE was applied to the DPV parameters for both aGCE and aSPCE. Pulse amplitude (E_{pulse}), pulse length (t_{pulse}), and scan rate (SC) were assessed on three levels each, and a central composite faced design was applied. The values of the parameter corresponding to the three levels considered are reported in Table 2. Fourteen experiments are required by design. All experiments were conducted in triplicate, taking the height of the current peak as an experimental response. The response obtained with the central point was used to validate the mode. The measurements were conducted on the following solutions: 3.0–30 μg L^{-1} DCF in 2.0 × 10^{-2} mol L^{-1} phosphate buffer at pH 2.5 for aGCE; 147 μg L^{-1} DCF in 1.0 × 10^{-1} mol L^{-1} phosphate buffer at pH = 2.0, for aSPCEs.

Table 2. Values of the applied measurement parameters the Design of Experiments and optimized parameters.

Parameter [a]	aGCE				aSPCE1			
	Level			Optimized	Level			Optimized
	−1	0	1		−1	0	1	
E_{pulse} (mV)	30	90	140	115	50	100	150	100
t_{pulse} (ms)	20	40	60	50	10	30	50	10
SC (mV/s)	10	25	40	25	10	25	40	25

[a] E_{pulse}: pulse amplitude; t_{pulse}: pulse length; SC: scan rate.

Data were processed by R-based CAT (Chemometric Agile Tool) software (http://gruppochemiometria.it/index.php/software, accessed on 15 November 2019).

3. Results

3.1. Characterization of DCF Electrochemical Behavior

Cyclic Voltammetry (CV) and Differential Pulse Voltammetry (DPV) were used to study the electrochemical reactivity of DCF on the surfaces of the activated electrodes and to evaluate the best pH and medium conditions for its determination.

The electrochemical activation, previously developed with GCE in order to enhance the acetaminophen (APAP) signals [20], was optimized for SPCEs. The best procedure was described in the experimental section. By this electrochemical activation, it is possible to obtain a systematic increase in the DCF peak currents, but the effect is quite moderate compared to that achievable for APAP. Moreover, the shift towards lower potential values of the APAP oxidation peak was not observed for DCF. An example of the voltammograms obtained from the DCF and acetaminophen solutions with SPCE and aSPCE is reported in Figure 1.

In order to study the pH effect on the DCF electrochemical signals, CV scans were carried out with aGCE on solutions of 20 μg L^{-1} DCF at different pH and medium: pH 2.0, with 1 × 10^{-2} mol L^{-1} hydrochloric acid; pH 2.0, with 2.5 × 10^{-2} mol L^{-1} phosphoric acid; pH 4.7, with 2.5 × 10^{-2} mol L^{-1} acetic buffer; pH 7.0, with 2.5 × 10^{-2} mol L^{-1} phosphate buffer. The signals obtained are reported in the Supporting Material File, Figure S1. The maximum values of the peak current were obtained with hydrochloric acid and phosphoric acid at pH 2.0. At this pH, the voltammograms show three well-defined peaks, the first one, corresponding to a non-reversible process, at about 0.85 V, and the other two, corresponding to a quite reversible process, in the potential range 0.3–0.4 V. Two very weak further peaks can be seen at about 0.62 V. Figure 2a shows the result of the first and the second CV scans on the same solution of 20 μg L^{-1} DCF, in 1 × 10^{-2} mol L^{-1} phosphoric buffer, pH = 2.0. In the first oxidative scan, only the peak at 0.85 V is visible; therefore, the other peaks are

probably due to DCF oxidation by-products. The reaction steps involved were named E and C to distinguish, respectively, electrochemical and chemical reactions and were depicted in Figure 2b for the main peaks. A chemical reaction occurs after the oxidation of DCF. This chemical reaction generates an electroactive species T and two distinct redox reactions therefore occur. The product of the chemical reaction T generates the electrochemical signals observable on the second scan at potentials between 0.3 and 0.4 V. Scheme 1 shortly describes the whole process:

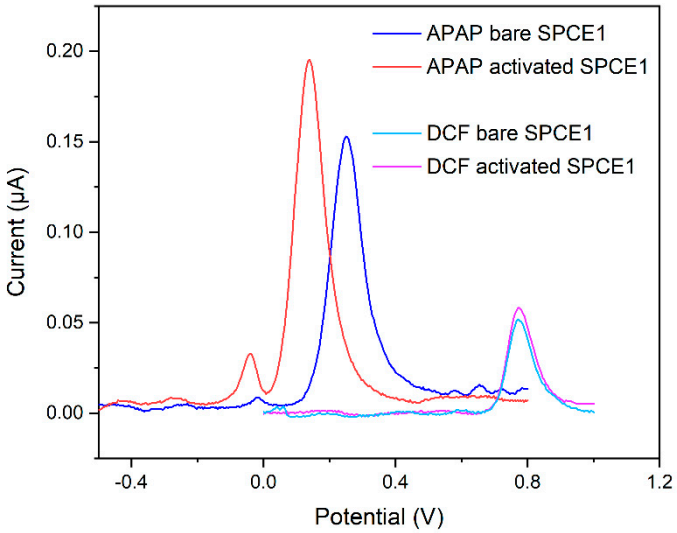

Figure 1. DPV signals of acetaminophen (APAP) and DCF obtained by non-activated and activated SPCE1. DPV signals of 11.5 mg L^{-1} acetaminophen in $4.5 \cdot 10^{-2}$ mol L^{-1} PB, pH 5.0, *E* vs. Ag/AgCl, E_{pulse} 100 mV, t_{pulse} 20 ms, E_{step} 4 mV, scan rate 5 mV/s. DPV signals of 4.0 mg L^{-1} DCF in $4.5 \cdot 10^{-2}$ mol L^{-1} PB, pH 2.0, *E* vs. Ag/AgCl; E_{pulse} 55 mV; t_{pulse} 25 ms; E_{step} 5 mV; scan rate 10 mV/s.

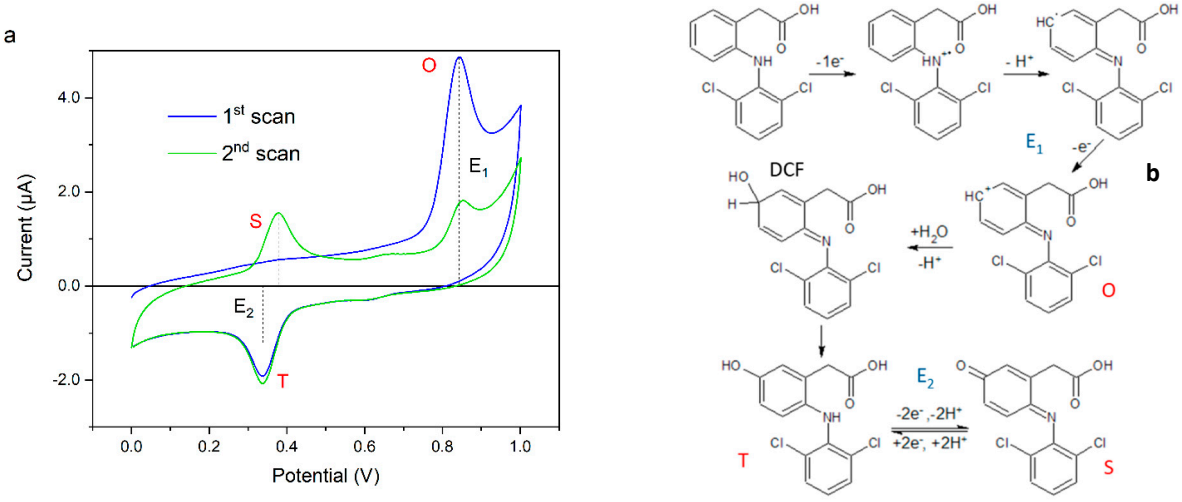

Figure 2. (**a**) Consecutives CV scans (aGCE) of 20 μg L^{-1} DCF in 1×10^{-2} mol L^{-1} phosphoric buffer, pH = 2.0; (**b**) Redox electrochemical-chemical (E1C1E2) mechanism of DCF [8].

Electrochemical process (E_1): DCF ⇆ O + $2e^-$
Chemical process (C): O → T
Electrochemical process (E_2): T ⇆ S + $2e^-$

Scheme 1. Redox electrochemical-chemical ($E_1C_1E_2$) mechanism of DCF.

The results are in agreement with those obtained by Goyal et al. [8] with an edge plane pyrolytic graphite sensor. They also revealed a drop in the oxidation peak current along with an appearance of an anodic peak of the species S and explained this by supposing the strong adsorption of the reaction products of DCF, which blocks the electrode surface and reduces the effective reaction sites at the modified electrode. This last statement is in accordance with our observations: the peak current due to the by-product increases with increasing the scan rate, but the peak separation between the reversible couple does not remain constant, suggesting that the electrode process is adsorption controlled. Furthermore, the peak due to the oxidation of DCF does not increase proportionally with the concentration of DCF in solution, nor does it increase the scan rate, and its height changes by replicating the measurements in the same solution, suggesting the presence of a disturbance process of the measurement.

Since the peaks due to the by-product show a more regular behavior, only the reduction peak of the by-product was considered for DCF quantification with aGCE, and the measurement conditions at pH 2.0 in 2.5×10^{-2} mol L^{-1} phosphoric acid were deemed the optimal ones, despite the greater peak height observed with hydrochloric acid, because of the low background signal and the good shape of the detectable peaks (see Figure S1).

The CV scans recorded with aSPCE are very similar to the ones obtained with aGCE. Indeed, the plots show three peaks: the first one is at 0.85 V, due to the oxidation of DCF, and then the other two peaks, an anodic one at about 0.55 V and a cathodic one at 0.50 V. These two peaks are related to the chemical reaction that occurs after DCF oxidation, with the production of a by-product, as seeable in Figure 2b.

The difference between the aGCE and the aSPCE lies in the interaction of the oxidation by-product with the electrode surface. In the case of aSPCE, the adsorption process is less important, and this leads to a regular increase in the peak current intensity due to the oxidation of DCF with increasing concentration of the analyte. Therefore, with aSPCE, the peak considered for the quantification of DCF is the one at 0.85 V due to the direct oxidation of DCF. After these observations, we set the working procedure in order to obtain the best linear response: for the aGCE, we decided to oxidize DCF by an anodic potential (0.8 V for 30 s) and then measure the reduction peak of its by-product adsorbed on the electrode surface; on the other hand, for the aSPCEs, the determination is pursued by the direct analysis of the solution without a pre-oxidation/adsorption process.

3.2. Characterization of Activated SPCE Surface

The surface of the GCE was previously studied [20], whereas the characterization of the surface of the SPCEs, before and after the electrochemical activation, was performed in this study by the Field Emission Scanning Electron Microscope-FE-SEM-TESCAN (Kohoutovice, Czech Republic) S9000G. FE-SEM images showed important morphological changes upon electrode polishing with alumina–water dough. After the treatment, the surface appears remarkably smoothed and less porous (Figure 3). This outcome is in accordance with the observation that the voltammetric signals obtained by the polished SPCEs are significantly more stable and well-shaped than those obtained without the surface treatment. The electrochemical activation process does not significantly change the surface morphology or the elemental composition, as is possible to note by comparing with Figure 3d,e and by the EDS results reported in Figure 4. This behavior is quite different from that observed in the case of GCE, for which the XPS spectra showed a massive increase in the oxygen bound to the electrode surface after the activation [20]. This may be the reason why the activation process performed on the SPCE shows a lower impact on the electrochemical signal of APAP if compared with that obtained with the GCE.

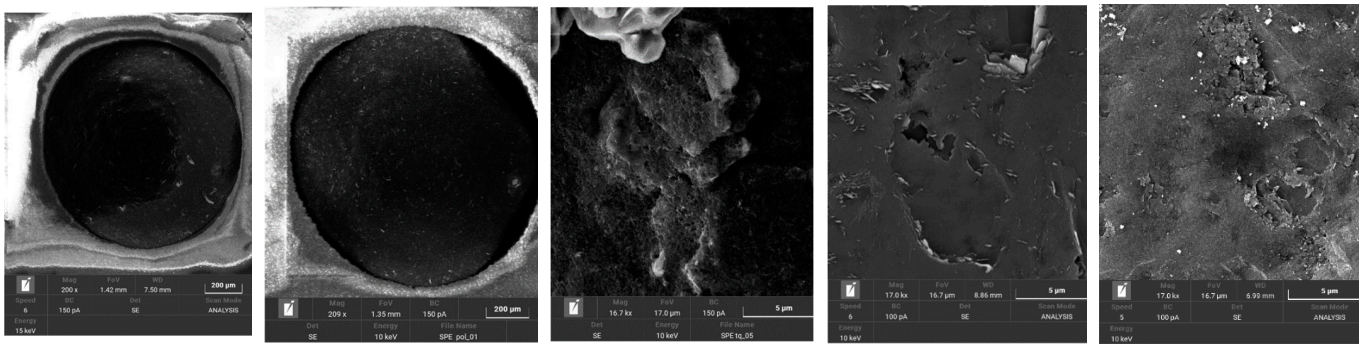

(**a**) (**b**) (**c**) (**d**) (**e**)

Figure 3. FE-SEM images of the SPCE1′s WE before the polishing procedure (**a**,**c**), after the polishing procedure (**b**,**d**), and after the electrochemical activation (**e**). (**a**,**b**) 10 keV; FOV(Field Of View) = 1.35 µm; (**c**–**e**) 10 keV; FOV = 17.00 µm.

bare SPCE1's WE polished SPCE1's WE activated SPCE1's WE

Element	Wt%	σ	Wt%	σ	Wt%	σ
C	84.5	0.3	86.2	0.4	92.5	0.2
O	11.1	0.3	10.4	0.3	4.1	0.1
Cl	4.4	0.1	3.4	0.1	3.4	0.2

Figure 4. EDS signals (5 keV) and weight percentage of the elements obtained analyzing the SPCE1 WE surface before the polishing procedure, after the polishing procedure, and after the electrochemical activation.

3.3. Design of Experiments Outcome

3.3.1. Design of Experiment Outcome with aGCE

The DoE procedure was applied to optimize the DPV parameters used for revealing the reduction peak of the DCF by-product. The sequence of experiments identified by the model was performed on three different days, running the series in a random way. All of the measurements were performed on a 0.02 mol L^{-1} phosphate buffer solution, at pH 2.5, by successive additions of DCF and exploring the signals in the concentration range 3.0–30 µg L^{-1}. The analytical response used for DoE was the mean current value obtained for a DCF solution of 12 µg L^{-1} (n = 3). The collected data were then processed with R software to estimate the model coefficients through Multiple Linear Regression (MLR) and generate the iso-response curves and response surfaces (Figure 5).

A first analysis of the confidence intervals of the model coefficients (Figure 5a), calculated with a confidence level of 95%, suggested that the terms containing the SC were not significant. The highest currents are obtained with a high value of E_{pulse} and a low value of t_{pulse}, as expected for DPV measurements (Figure 5b), but the maximum response was obtained for parameter values located at the border of the investigated ranges. Unfortunately, near these conditions, the precision of the measurement decreases. This is evident by observing the standard deviation values obtained for the different experiments conducted for the DoE, reported in Figure 6, and by the results obtained applying the DoE to the standard deviation values (Figure S3). Considering this issue, the experimental conditions

that were chosen as optimal (see Table 2 and Figure S4) were a compromise between a high current value and a good precision of the measurement and which led to the achieveement of satisfactory sensitivity and repeatability (red bar in Figure 6).

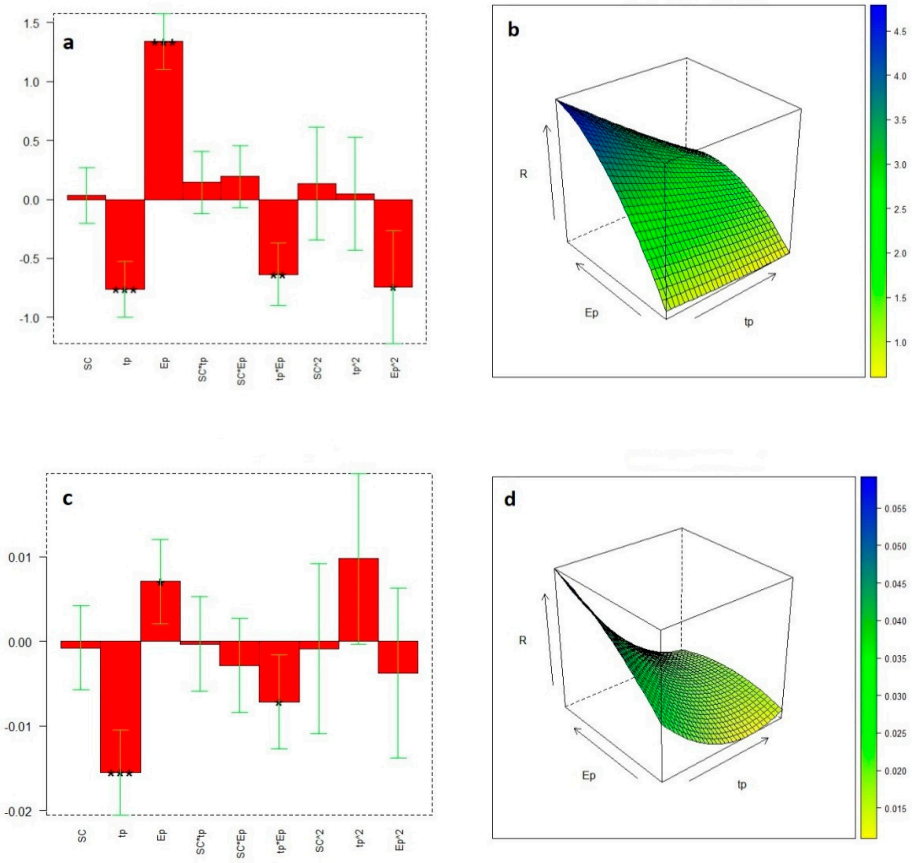

Figure 5. Design of Experiment: (**a**,**c**) coefficients of the model obtained with aGCE (**a**) and aSPCE (**c**) (significance level = 0.05; * = $p \leq 0.05$; ** = $p \leq 0.01$; *** = $p \leq 0.001$); (**b**,**d**) response surfaces obtained with SC 25 mV s^{-1} with aGCE (**b**) and aSPCE (**d**). $E_p = E_{pulse}$; $t_p = t_{pulse}$.

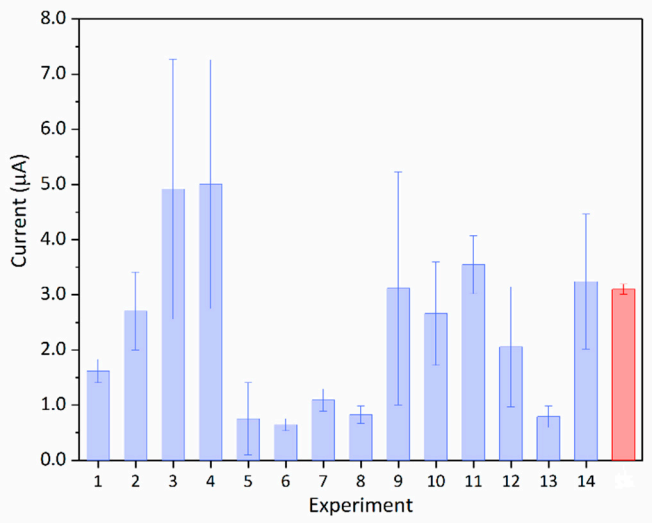

Figure 6. Mean current intensity and the corresponding standard deviation calculated on the three measurement replicates of each DoE experiment conducted with the aGCE. The red bar identifies the measurement results obtained with optimized conditions.

3.3.2. Design of Experiment Outcome with aSPCE

The DoE procedure was applied to optimize the DPV parameters used for revealing the oxidation peak of DCF. The sequence of experiments identified by the model was performed on three different days, using three different aSPCEs, and running the experimental series in a random way. All of the measurements were performed on a 0.1 mol L^{-1} phosphate buffer solution at pH 2.0, and the analytical response used for DoE was the mean current value obtained for a solution 147 μg L^{-1} DCF. The collected data were then processed with R software to estimate the model coefficients through Multiple Linear Regression (MLR) and generate the iso-response curves and response surfaces (Figure 5). As for the aGCE, the analysis of the confidence intervals of the model coefficients (Figure 5c), calculated with a confidence level of 95%, suggested that the terms containing the SC were not significant. The maximum response was obtained for parameter values located at the border of the investigated ranges (Figure 5d), but for high E_{pulse} values, the noise noticeably increases; therefore, it was chosen to work with a medium value of E_{pulse} and a low value of t_{pulse}, as reported in Table 2 and shown in Figure S4.

3.4. Differential Pulse Voltammetry

3.4.1. Analysis with the aGCE

The DPV analyses with aGCE, as previously written, were performed measuring the reduction peak of the by-product. The measurements were carried out in two steps:(i) the DCF was first electrochemically oxidized and transformed into its by-product by the application of an anodic potential; the DCF by-product generated was adsorbed onto the electrode surface; (ii) a cathodic potential scan was then performed with the aGCE immersed in a blank solution, after washing with ultrapure water. The parameters used for the anodic preconditioning: medium 5×10^{-2} mol L^{-1} H_3PO_4/KH_2PO_4 (pH 2.0) with different DCF concentrations (3–30 μg L^{-1}); potential applied: 0.8 V, conditioning time: 30 s. The parameter used for the potential cathodic scan were those optimized by the DoE procedure (Table 2).

Figure 7a shows the DPV voltammograms obtained for DCF concentrations included between 3 and 30 μg L^{-1}. To evaluate the stability of the signals, for each concentration level, the measurement was repeated three times. Figure 7b shows the current values obtained by increasing the DCF concentration. In this case, four independent replicates, with one measurement for each concentration level, have been performed. It can be seen that the trend is linear up to a DCF concentration of 16 μg L^{-1}, after which the saturation of the electrode surface occurs, as expected when an adsorption process is involved. Figure 7c shows the linear fit obtained in the linearity range, and the inset Table shows the fit parameters.

From the plots shown in Figure 7c, the mean values of LoD (limit of detection) and LoQ (limit of quantification) were estimated by the standard deviation of the intercepts defined by the ordinary linear regressions. The LoD and LoQ values correspond to the analyte amount for which the current signal is equal to 3.3 times or 10 times the standard deviation of the intercepts, respectively. The estimated values of the LoD and LoQ were, respectively, 1.6 μg L^{-1} and 4.8 μg L^{-1}.

3.4.2. Analysis with aSPCEs

The determination of the concentration of DCF by SPCE electrodes, as previously reported, was obtained through the measurement of the DCF oxidation peak current. In particular, analyses were performed both by immersing the electrode in the solution or by deposing a drop of solution on the electrode.

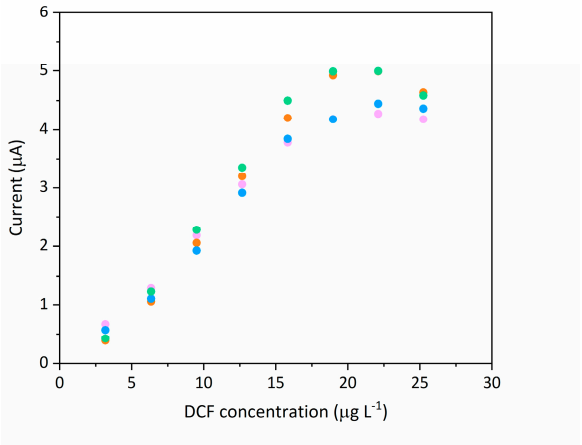

(**a**)

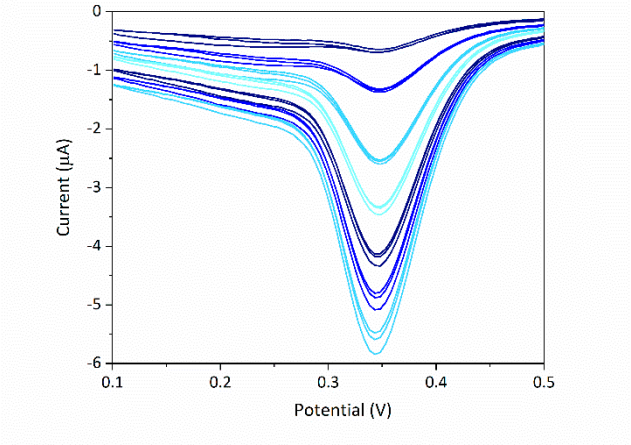

(**b**)

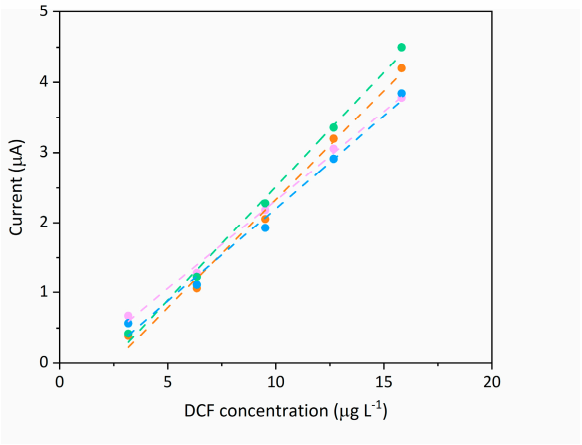

(**c**)

Exp.	Linear Fit Parameters				
	Slope	**Std. err.**	**Intercept**	**Std. err.**	**R^2**
1	0.325	0.012	−0.73	0.12	0.9961
2	0.309	0.015	−0.76	0.16	0.9926
3	0.264	0.016	−0.44	0.17	0.9889
4	0.253	0.008	−0.21	0.09	0.9965

(**d**)

Figure 7. (**a**) Reduction peaks obtained by DPV on the DCF by-product adsorbed on the aGCE surface (3-22 µg L^{-1} DCF; PB 5 × 10^{-2} mol L^{-1} pH 2.0; E vs. Ag/AgCl; three replicates for each concentration level); (**b**) current signals obtained for each concentration level (four independent replicates, one measurement for each concentration level); (**c**) linear fit of signals of DCF in the concentration range 3–16 µg L^{-1}; (**d**) Linear fit parameters estimated on the DPV signals of DCF by-product adsorbed on the aGCE surface (3–16 µg L^{-1} DCF; PB 5 × 10^{-2} mol L^{-1} pH 2).

Solution Analysis

Analyses were performed using two aSPCEs purchased from different companies in order to evaluate whether there were any differences in the analytical response.

The measurements performed with the aSPCE1 showed good linearity in the concentrations range between 20 and 146 µg L^{-1}, as we can see in Figure 8a,c. Figure 8c shows three calibration lines obtained on three different days using three different electrodes, indicating the good repeatability of the measurement. The peak heights used for the linear fits were estimated by baseline subtraction. The signals obtained with the aSPCE2 show a higher current value with respect to the signals obtained with aSPCE1, as expected based on the size of the surface area of the WE, but the peaks are not well defined and repeatability is lower. The linear fit parameters are collected in Table 3.

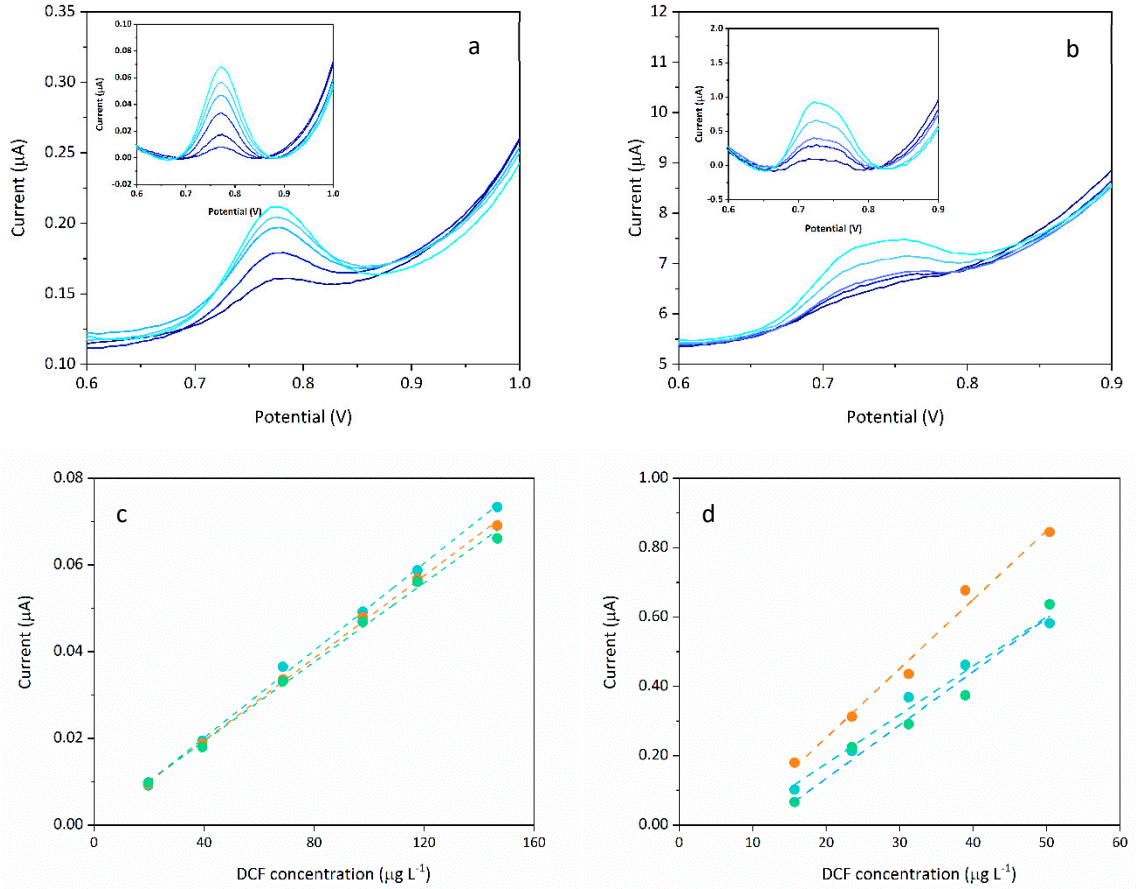

Figure 8. (**a**) Peaks obtained by solution DPV analysis with aSPCE1 on 20–146 μg L^{-1} DCF solutions (1.0 × 10^{-1} mol L^{-1} PB, pH 2.0; E vs. Ag/AgCl); the inset graph shows the peaks after baseline subtraction; (**b**) Peaks obtained by solution DPV analysis with aSPCE2 on 15–50 μg L^{-1} DCF solutions (1.0 × 10^{-1} mol L^{-1} PB, pH 2.0; E vs. Ag/AgCl); the inset graph show the peaks after baseline subtraction; (**c**) linear fit of signals recorded by solution DPV analysis with aSPCE1 on 20–146 μg L^{-1} DCF solutions; (**d**) linear fit of signals recorded by solution DPV analysis with aSPCE2 on 15–50 μg L^{-1} DCF solutions.

Table 3. Linear fit parameters estimated on current signals recorded by solution and drop DPV analysis with aSPCE.

Electrode	Linear Fit Parameters				
	Solution Analysis				
aSPCE-1	**Slope**	**Std. err.**	**Intercept**	**Std. err.**	**R^2**
1	5.03×10^{-4}	1.0×10^{-5}	-2.13×10^{-5}	9.6×10^{-4}	0.9983
2	4.75×10^{-4}	7.9×10^{-6}	4.48×10^{-4}	7.4×10^{-4}	0.9989
3	4.56×10^{-4}	1.3×10^{-5}	1.09×10^{-3}	1.25×10^{-3}	0.9965
aSPCE-2	**Slope**	**Std. err.**	**Intercept**	**Std. err.**	**R^2**
1	1.41×10^{-2}	1.0×10^{-3}	-1.05×10^{-1}	3.5×10^{-2}	0.9840
2	1.99×10^{-2}	1.4×10^{-3}	-1.46×10^{-1}	4.8×10^{-2}	0.9851
3	1.54×10^{-2}	1.6×10^{-3}	-1.74×10^{-1}	5.4×10^{-2}	0.9695
	Drop analysis				
aSPCE-1	**Slope**	**Std. err.**	**Intercept**	**Std. err.**	**R^2**
1	3.68×10^{-4}	6.5×10^{-6}	-2.72×10^{-3}	5.4×10^{-4}	0.9991
2	3.19×10^{-4}	1.1×10^{-5}	-8.45×10^{-4}	8.2×10^{-4}	0.9967
3	2.68×10^{-4}	8.9×10^{-6}	-2.04×10^{-3}	6.9×10^{-4}	0.9967
aSPCE-2	**Slope**	**Std. err.**	**Intercept**	**Std. err.**	**R^2**
	1.31×10^{-2}	7.4×10^{-4}	-3.17×10^{-1}	7.2×10^{-2}	0.9975
	7.83×10^{-3}	3.0×10^{-4}	-1.85×10^{-1}	2.9×10^{-2}	0.9956
	1.33×10^{-2}	6.1×10^{-4}	-2.52×10^{-1}	5.9×10^{-2}	0.9938

From the plots shown in Figure 8c,d, the mean values of LoD and LoQ were estimated by the standard deviation of the intercepts defined by the ordinary linear regressions. The LoD and LoQ values correspond to the analyte amount for which the current signal is equal to 3.3 times or 10 times the standard deviation of the intercepts, respectively. The value of the LoD and LoQ estimated for aSPCE1 and aSPCE2 were, respectively, 7 μg L^{-1} and 20 μg L^{-1}, and 9 μg L^{-1} and 28 μg L^{-1}.

Drop Analysis

After the solution analysis, we performed a drop analysis. This way of operating takes advantage of the configuration of the SPCEs, which have all the electrodes (reference, working, and auxiliary) printed on the same planar support. Thus, instead of dipping the electrode into a solution, we can deposit a single drop that covers all the electrodes and on which we can perform the analysis. The drop has a definite volume: for aSPCE1, it was 60 μL, while for aSPCE2, it was 90 μL due to its higher WE surface.

After every analysis, we washed the electrode with ultrapure water, and then, before the following analysis, we conditioned the aSPCEs by immersion into the blank solution under stirring for a few seconds. This procedure ensures good interaction of the drop with the electrode-active surface.

Drop analysis could be very useful because it can provide a lot of measures with small volumes of the sample. For a better analysis, in this case, we have to set an equilibration time of 90 s for aSPCE1 and 150 s for aSPCE2. This time allows the correct diffusion of the analyte to the working electrode surface, enhancing the ability of the aSPCEs to detect DCF.

Similar to the solution analysis case, the values of LoD and LoQ were estimated by the standard deviation of the intercepts defined by ordinary linear regressions. Figure 9a shows the plots used for the aSPCE1, while Figure 9b shows the plots used for the aSPCE2. The peak heights used for the linear fits were estimated by baseline subtraction.

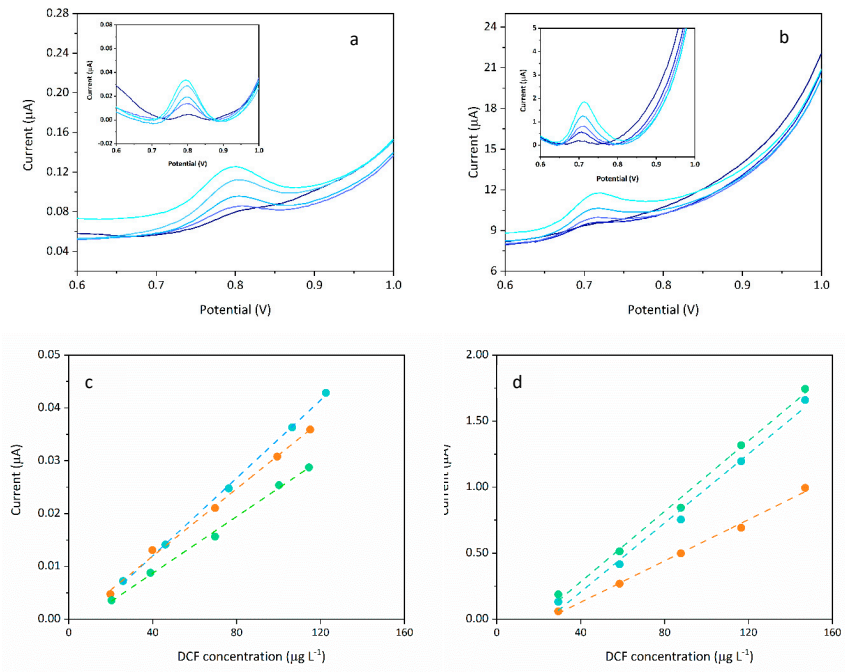

Figure 9. (**a**) Peaks obtained by drop DPV analysis with aSPCE1 on 25–120 μg L^{-1} DCF solutions (1.0×10^{-1} mol L^{-1} PB, pH 2.0; E vs. Ag/AgCl); the inset graph shows the peaks after baseline subtraction; (**b**) Peaks obtained by drop DPV analysis with aSPCE2 on 29–147 μg L^{-1} DCF solutions (1.0×10^{-1} mol L^{-1} PB, pH 2.0; E vs. Ag/AgCl); the inset graph show the peaks after baseline subtraction; (**c**) linear fit of signals recorded by drop DPV analysis with aSPCE1 on 25–120 μg L^{-1} DCF solutions; (**d**) linear fit of signals recorded by drop DPV analysis with aSPCE2 on 29–147 μg L^{-1} DCF solutions.

The value of the LoD and LoQ estimated for aSPCE1 and aSPCE2 were, respectively, 9 μg L^{-1} and 28 μg L^{-1}, and 15 μg L^{-1} and 45 μg L^{-1}.

The first observation is that both the aSPCEs have higher values of LoD and LoQ for a drop analysis than for a solution analysis owing to the greater variability in peak heights. The aSPCE1, however, continues to provide better results than the aSPCE2, having the ability to detect lower concentrations of DCF.

4. Discussion

The electrochemical behavior of DCF was studied on GCE and SPCE after the anodic activation. This approach allowed us to explore the analytical response of the two electrode types to DCF, highlight the differences between the two devices, and optimize the measurement conditions for both electrode types. On both kinds of electrodes, the electrochemical response of DCF is not reversible. DCF signals showed to be enhanced by the anodic activation of the electrode surface, even if to a lesser extent than other previously investigated drugs and acid pH. Moreover, DCF and its by-products tend to be adsorbed on the surfaces; in particular, the by-products can be easily adsorbed on the activated surface of the GCE. From this point of view, the behavior of DCF on activated GCE and SPCEs is different. The measures showed that by using SPCEs, we obtain a linear relationship between the concentration of DCF and its anodic current, while this is not possible for GCE on which the adsorption of the by-products is significant. With GCE, it was possible to work in linear conditions exploiting the pre-adsorption of the oxidation by-product on the electrode surface.

Despite the fact that the SPEs were supplied as ready-for-use, we observed that the preliminary polishing process by alumina–water dough, commonly used for the solid electrodes, smooths the electrode surface and significantly stabilizes the electrochemical signals. The polishing process can be conducted only once, before the measurement, since the SPE is considered to be a disposable device and was discarded after the measurement.

By both GCE and SPCE, it was possible to find conditions for which the current signals linearly increase with DCF concentration and to estimate the limit parameters. SPCEs from two different suppliers were tested, and the best performance was obtained with the SPCE1. The different performances can be accounted for by the smallest WE surface of SPCE1 or by the difference in the ink composition. The GCE showed lower limit parameters and better repeatability with respect to SPCEs. The limit parameters defined for both GCE and SPCEs are lower or similar to those reported in the scientific literature (see Table 1), except for the case studied by Sasal et al. [18,19], who modified the electrode surface with carboxyl functionalized multi-walled carbon nanotubes.

The quality of the signals and the concentration range obtained by aGCE are quite satisfactory but operating by adsorption presents some concerns. In fact, if we consider the use of real samples, the adsorption phase can also involve the matrix, with possible arising of interferences or reduction in the sensibility by the saturation of the active surface of the WE. Another fact to take into account is that DCF is well adsorbed on many surfaces, so the polishing step before every single measurement has to be very careful in order to avoid memory effect due to previous measures. The process is rather tedious and non-automatable and causes the analytical method to be unsuitable for screening analyses. These issues can be well avoided by the adoption of a different kind of electrode, such as the SPCE. The use of SPCE may have some other advantages. In fact, by SPCE, it is possible to directly measure the current due to DCF's oxidation without a preliminary adsorption step. Moreover, SPCEs are disposable devices; therefore, it is possible to avoid the risk of memory effects, polishing, and electrode treatment between successive measurements, and they allow the consumption of small sample volumes. Therefore, SPCEs may be particularly suitable for screening analysis in order to process many samples in a very short time.

Supplementary Materials: The following supporting information can be downloaded at: https://www.mdpi.com/article/10.3390/app12167983/s1. Figure S1: CV scans (scan rate 0.05 V/s, 7th scan) of DCF 20 mg L^{-1} as a function of pH and buffer type; Figure S2: Contour plots obtained by the Design of experiments applied to the measurements with aGCE (a) and with aSPCE (b) (SC 25mV s^{-1}). $E_p = E_{pulse}$; $t_p = t_{pulse}$; Figure S3: Results of the Design of experiments conducted using as response the standard deviation values obtained for the different experiments performed with the aGCE: (a) coefficients of the model; (b) response surfaces (SC 25mV s^{-1}); (c) contour plot (SC 25mV s^{-1}). $E_p = E_{pulse}$; $t_p = t_{pulse}$; Figure S4: Position of the optimized measurement conditions (blue dot) in the experiment space defined by the central composite faced design (a: aGCE; b: aSPCE).

Author Contributions: Conceptualization, S.B. (Silvia Berto); methodology, S.B. (Silvia Berto), A.G. and M.M.; investigation, E.C., G.A., E.T. and P.I.; resources, E.P., M.M. and O.A.; data curation, E.C. and S.B. (Silvia Berto); writing—original draft preparation, S.B. (Silvia Berto); writing—review and editing, S.B. (Silvia Berto), E.C. and E.P.; visualization, S.B. (Stefano Bertinetti) and E.C.; supervision, S.B. (Silvia Berto) and O.A.; project administration, O.A.; funding acquisition, O.A. All authors have read and agreed to the published version of the manuscript.

Funding: This research was financially supported by the MIUR/PNRA program in the framework of the PNRA project PNRA18_00216-B2 entitled "Emerging contaminants in the Ross Sea: occurrence, sources and ecotoxicological risks".

Institutional Review Board Statement: Not applicable.

Informed Consent Statement: Not applicable.

Data Availability Statement: Data are contained within the article.

Conflicts of Interest: The authors declare no conflict of interest.

References

1. Acuña, V.; Bregoli, F.; Font, C.; Barceló, D.; Corominas, L.; Ginebreda, A.; Petrovic, M.; Rodríguez-Roda, I.; Sabater, S.; Marcé, R. Balancing the health benefits and environmental risks of pharmaceuticals: Diclofenac as an example. *Environ. Int.* **2015**, *85*, 327–333. [CrossRef]
2. Zhang, Y.; Geißen, S.U.; Gal, C. Carbamazepine and diclofenac: Removal in wastewater treatment plants and occurrence in water bodies. *Chemosphere* **2008**, *73*, 1151–1161. [CrossRef] [PubMed]
3. Loos, R.; Marinov, D.; Sanseverino, I.; Napierska, D.; Lettieri, T. *Review of the 1st Watch List under the Water Framework Directive and Recommendations for the 2nd Watch List*; EUR 29173 EN; Publications Office of the European Union: Luxembourg, 2018. [CrossRef]
4. Risebrough, R. Fatal medicine for vultures. *Nature* **2004**, *427*, 596–598. [CrossRef] [PubMed]
5. Oaks, J.L. Diclofenac residues as the cause of vulture population decline in Pakistan. *Nature* **2004**, *427*, 630–633. [CrossRef] [PubMed]
6. Commission Implementing Decision (EU). 2015/495 of 20 March 2015 establishing a watch list of substances for Union-wide monitoring in the field of water policy pursuant to Directive 2008/105/EC of the European Parliament and of the Council. *Off. J. Eur. Union* **2015**, *L78/40*, 20–30.
7. Tavazzi, S.; Paracchini, B.; Suurkuusk, G.; Mariani, G.; Loos, R.; Ricci, M.; Gawlik, B.M. *Water Framework Directive. Watch List Method. Analysis of Diclofenac in Water*; EUR 26902; Publications Office of the European Union: Luxembourg, 2014. [CrossRef]
8. Goyal, R.N.; Chatterjee, S.; Agrawal, B. Electrochemical investigations of diclofenac at edge plane pyrolytic graphite electrode and its determination in human urine. *Sens. Actuators B Chem.* **2010**, *145*, 743–748. [CrossRef]
9. Arvand, M.; Gholizadeh, T.M.; Zanjanchi, M.A. MWCNTs/$Cu(OH)_2$ nanoparticles/IL nanocomposite modified glassy carbon electrode as a voltammetric sensor for determination of the non-steroidal anti-inflammatory drug diclofenac. *Mater. Sci. Eng. C* **2012**, *32*, 1682–1689. [CrossRef] [PubMed]
10. Mokhtari, A.; Karimi-Maleh, H.; Ensafi, A.A.; Beitollahi, H. Application of modified multiwall carbon nanotubes paste electrode for simultaneous voltammetric determination of morphine and diclofenac in biological and pharmaceutical samples. *Sens. Actuators B Chem.* **2012**, *169*, 96–105. [CrossRef]
11. Ensafi, A.A.; Izadi, M.; Karimi-Maleh, H. Sensitive voltammetric determination of diclofenac using room-temperature ionic liquid-modified carbon nanotubes paste electrode. *Ionics* **2013**, *19*, 137–144. [CrossRef]
12. Sarhangzadeh, K.; Khatami, A.A.; Jabbari, M.; Bahari, S. Simultaneous determination of diclofenac and indomethacin using a sensitive electrochemical sensor based on multiwalled carbon nanotube and ionic liquid nanocomposite. *J. Appl. Electrochem.* **2013**, *43*, 1217–1224. [CrossRef]
13. Goodarzian, M.; Khalilzade, M.A.; Karimi, F.; Gupta, K.V.; Keyvanfard, M.; Bagheri, H.; Fouladgar, M. Square wave voltammetric determination of diclofenac in liquid phase using a novel ionic liquid multiwall carbon nanotubes paste electrode. *J. Mol. Liq.* **2014**, *197*, 114–119. [CrossRef]

14. Fard, G.P.; Alipour, E.; Ali Sabzi, R.E. Modification of a disposable pencil graphite electrode with multiwalled carbon nanotubes: Application to electrochemical determination of diclofenac sodium in some pharmaceutical and biological samples. *Anal. Methods* **2016**, *8*, 3966–3974. [CrossRef]
15. Shalauddin, M.; Akhter, S.; Bagheri, S.; Abd Karim, M.S.; Adib Kadri, N.; Basirun, W.J. Immobilized copper ions on MWCNTS-Chitosan thin film: Enhanced amperometric sensor for electrochemical determination of diclofenac sodium in aqueous solution. *Int. J. Hydrogen Energy* **2017**, *42*, 19951–19960. [CrossRef]
16. Pourghobadi, R.; Baezzat, M.R. Silica nanoparticles modified carbon paste electrode as a voltammetric sensor for determination of diclofenac. *Anal. Bioanal. Chem. Res.* **2017**, *4*, 261–268. [CrossRef]
17. de Carvalho, R.C.; Betts, A.J.; Cassidy, J.F. Diclofenac determination using CeO2 nanoparticle modified screen-printed electrodes—A study of background correction. *Microchem. J.* **2020**, *158*, 105258. [CrossRef]
18. Sasal, A.; Tyszczuk-Rotko, K.; Wojciak, M.; Sowa, I.; Kurylo, M. Simultaneous Analysis of Paracetamol and Diclofenac Using MWCNTs-COOH Modified Screen-Printed Carbon Electrode and Pulsed Potential Accumulation. *Materials* **2020**, *13*, 3091. [CrossRef] [PubMed]
19. Sasal, A.; Tyszczuk-Rotko, K.; Wójciak, M.; Sowa, I. First electrochemical sensor (screen-printed carbon electrode modified with carboxyl functionalized multiwalled carbon nanotubes) for ultratrace determination of diclofenac. *Materials* **2020**, *13*, 781. [CrossRef] [PubMed]
20. Chiavazza, E.; Berto, S.; Giacomino, A.; Malandrino, M.; Barolo, C.; Prenesti, E.; Vione, D.; Abollino, O. Electrocatalysis in the oxidation of acetaminophen with an electrochemically activated glassy carbon electrode. *Electrochim. Acta* **2016**, *192*, 139–147. [CrossRef]
21. Berto, S.; Carena, L.; Valmacco, F.; Barolo, C.; Conca, E.; Vione, D.; Buscaino, R.; Fiorito, M.; Bussi, C.; Abollino, O.; et al. Application of an electro-activated glassy-carbon electrode to the determination of acetaminophen (paracetamol) in surface waters. *Electrochim. Acta* **2018**, *284*, 279–286. [CrossRef]

SUPPORTING MATERIALS

Voltammetric Study for the Determination of Diclofenac in Aqueous Solutions Using Electro-Activated Carbon Electrodes

Silvia Berto [1,*], Enrico Cagno [1], Enrico Prenesti [1], Giulia Aragona [1], Stefano Bertinetti [1], Agnese Giacomino [2], Paolo Inaudi [2], Mery Malandrino [1], Emanuele Terranova [1] and Ornella Abollino [2]

[1] Department of Chemistry, University of Turin, via P. Giuria 7, 10125 Turin, Italy
[2] Department of Drug Science and Technology, University of Turin, Via P. Giuria 9, 10125 Turin, Italy
* Correspondence: silvia.berto@unito.it

1. Cyclic Voltammetry

The CV signals were collected on solution of DCF 20 μg L^{-1} at different pH and medium: pH 2, with hydrochloric acid 1×10^{-2} mol L^{-1}; pH 2, with phosphoric acid 2.5×10^{-2} mol L^{-1}; pH 4.7, with acetic buffer 2.5×10^{-2} mol L^{-1}; pH 7, with phosphate buffer 2.5×10^{-2} mol L^{-1}. The signals obtained are reported Figure S1.

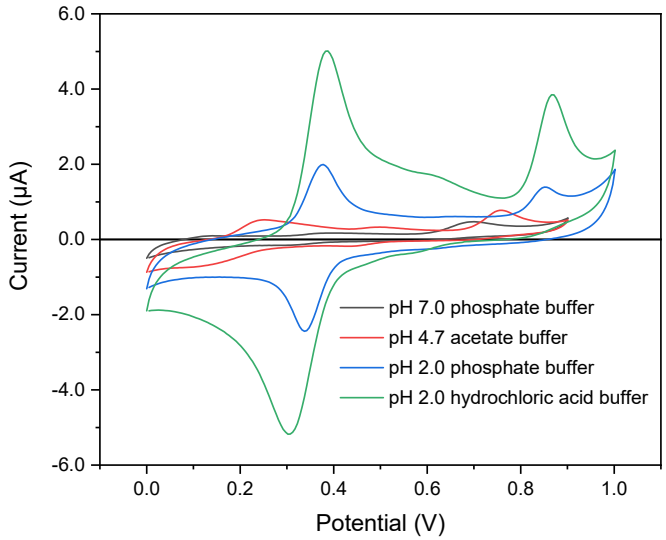

Figure S1. CV scans (scan rate 0.05 V/s, 7th scan) of DCF 20 mg L^{-1} as a function of pH and buffer type.

2. Design of Experiments outcome

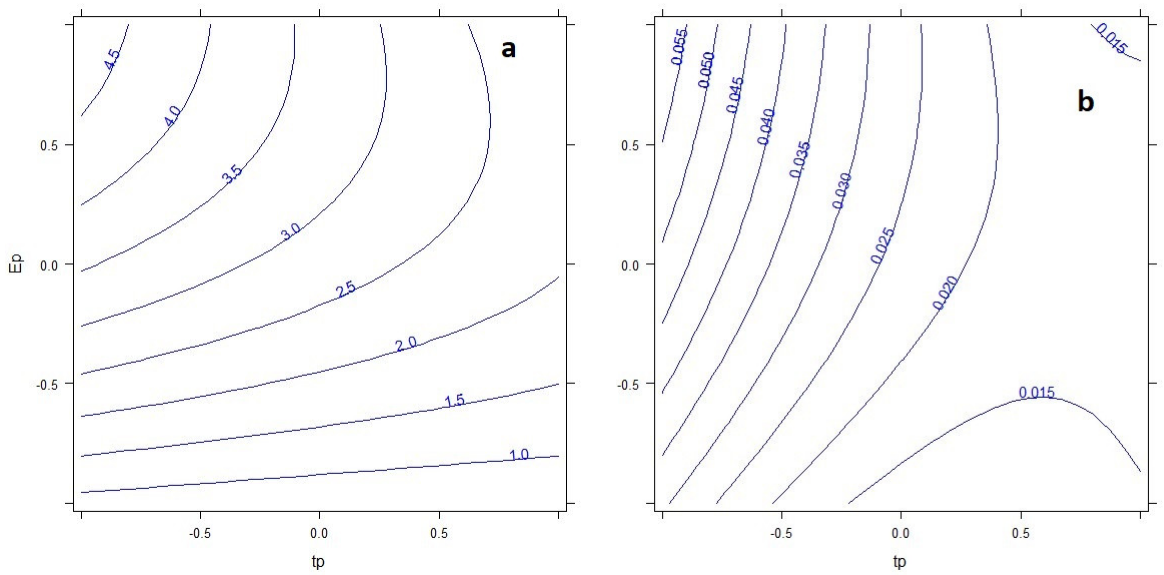

Figure S2. Contour plots obtained by the Design of experiments applied to the measurements with aGCE (**a**) and with aSPCE (**b**) (SC 25mV s^{-1}). $E_p = E_{pulse}$; $t_p = t_{pulse}$.

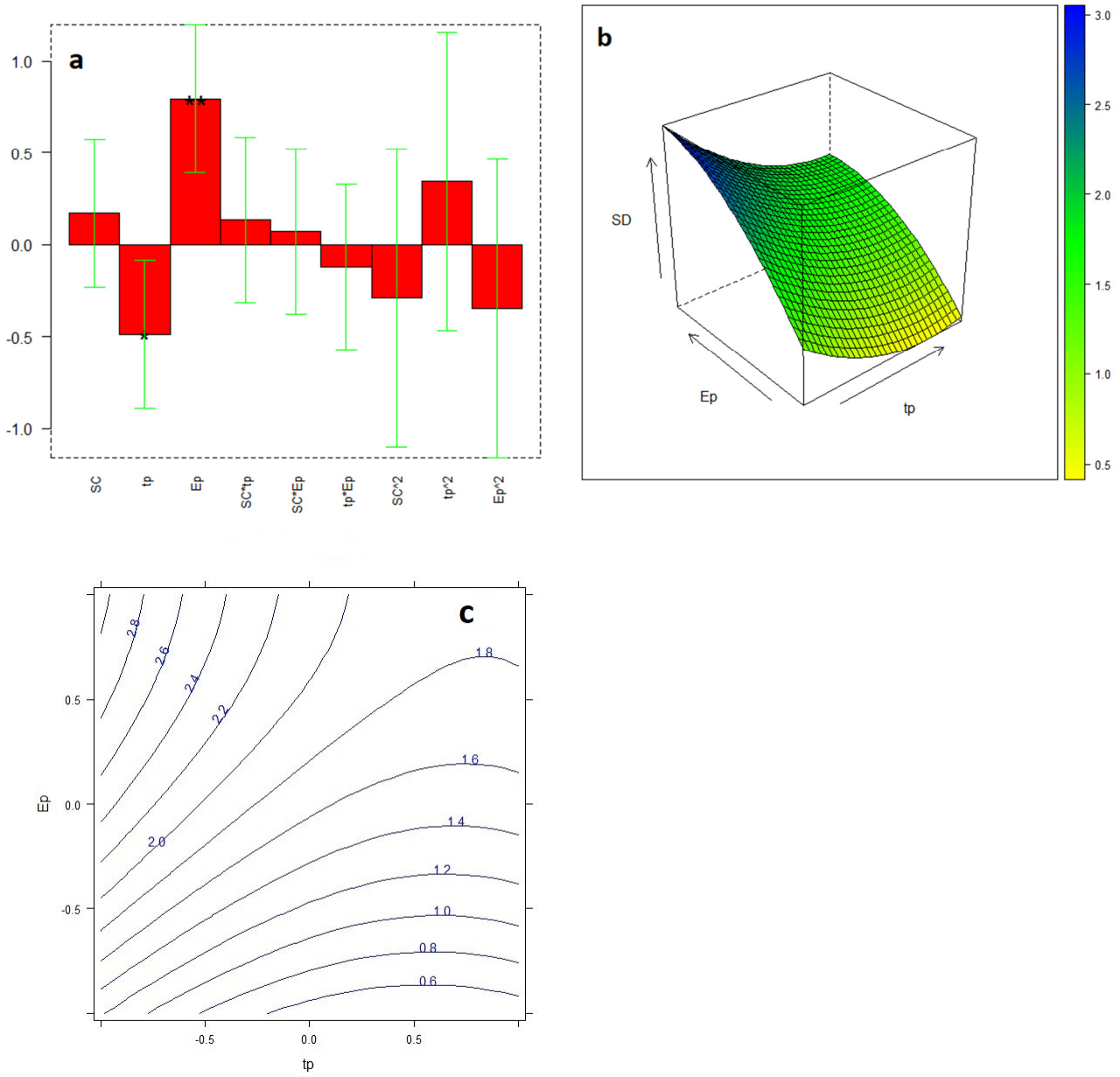

Figure S3. Results of the Design of experiments conducted using as response the standard deviation values obtained for the different experiments performed with the aGCE: (**a**) coefficients of the model; (**b**) response surfaces (SC 25mV s^{-1}); (**c**) contour plot (SC 25mV s^{-1}). $E_p = E_{pulse}$; $t_p = t_{pulse}$.

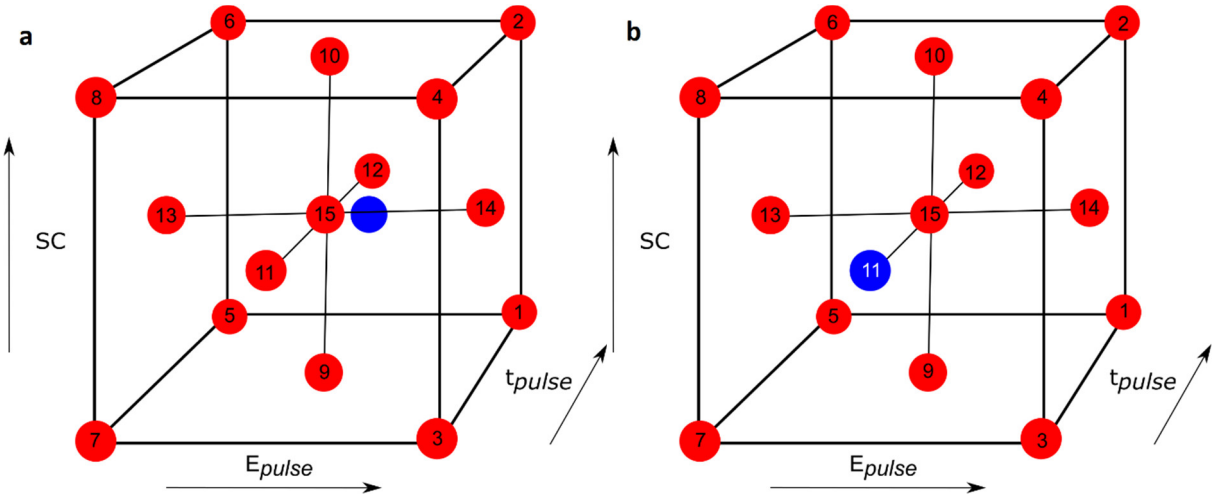

Figure S4. Position of the optimized measurement conditions (blue dot) in the experiment space defined by the central composite faced design ((**a**) aGCE; (**b**) aSPCE).